10.1071/WF19042_AC

International Journal of Wildland Fire **29**, 739–751

Supplementary Material

Modeling suppression difficulty: current and future applications

Francisco Rodríguez y Silva[A,D], Christopher D. O'Connor[B], Matthew P. Thompson[C], Juan Ramón Molina Martínez[A], David E. Calkin[B]

[A]Department of Forest Engineering, Forest Fire Laboratory, University of Córdoba, Edificio Leonardo da Vinci, Campus de Rabanales, E-14071 Córdoba, Spain.

[B]US Department of Agriculture Forest Service, Rocky Mountain Research Station, 800 East Beckwith Avenue, Missoula, MT 59801, USA.

[C]US Department of Agriculture Forest Service, Rocky Mountain Research Station, 240 West Prospect Road, Fort Collins, CO 80526, USA.

[D]Corresponding author. Email: ir1rosif@uco.es

S1: Equations to estimate rate of spread in canyons, as a function of fuel type

Variables specific to these calculations include the angle of opening α (separation between the two hillsides of the canyon), the steepness of side slopes β (angle), and wind speed in m/s (Um).

Grass equation:

$$R = 68.7066 + 0.0730920xUm - 0.0983203x\alpha + 0.882936x\beta$$

R squared: R^2=0.946522

R squared adjusted: R^2=0.944015

Timber litter equation:

$$R = 66.9502 + 0.228187xUm - 0.103230x\alpha + 1.20467x\beta$$

R squared: R^2=0.960888

R squared adjusted: R^2=0.959055

Shrub equation:

$$R = 67.4535 + 0.187718xUm - 0.101836x\alpha + 1.10639x\beta$$

R squared: R^2=0.957805

R squared adjusted: R^2=0.955827

Slash equation:

$$R = 68.7066 + 0.0730920xUm - 0.0983203x\alpha + 0.882936x\beta$$

R squared: R^2=0.946522

R squared adjusted: R^2=0.944015

S2: Categorization schemas for next-generation SDI

Table S2.1 provides six categories of SDI developed from field observations and feedback from wildfire professionals. Table S2.2 provides a more expansive chart that assigns the same categories to SDI values but expressed in relation to its subcomponents. Lastly, Table S2.3 provides a classification of canyons depending on the angles of opening angles of opening α (separation between the two hillsides of the canyon) and steepness of side slopes β.

Table S2.1. SDI classification thresholds

Categories	SDI intervals
Very low (vl)	0.02-0.32
Low (l)	0.33-0.60
Medium (m)	0.61-1
High (h)	1.01-1.5
Very High (vh)	1.51-10
Extreme (e)	11-30

Table S2.2. Categorical descriptions of SDI in relation to primary sub-components, Energy Release Component (I_{ce}) and the Suppression Opportunity Index (IS_{oi})

I_{ce}\IS_{oi}	50	45	40	35	30	25	20	15	10	5	1
30	l	l	m	h	h	h	h	vh	e	e	e
28	l	l	m	h	h	h	h	vh	e	e	e
26	l	l	m	h	h	h	h	vh	vl	e	e
24	l	l	m	h	h	h	h	vh	vl	e	e
22	l	l	l	m	h	h	h	vh	vl	e	e
20	l	l	l	m	h	h	h	vh	vl	e	e
18	l	l	l	m	m	h	h	h	vl	e	e
16	vl	l	l	m	m	m	h	h	vl	e	e
14	vl	vl	l	l	m	m	h	h	h	vl	e
12	vl	vl	vl	l	l	m	m	h	h	vl	e
10	vl	vl	vl	vl	l	l	m	h	h	vl	e
8	vl	vl	vl	vl	vl	l	m	h	m	h	e
6	vl	vl	vl	vl	vl	vl	l	h	m	m	e
4	vl	vl	vl	vl	vl	vl	vl	l	l	m	h
2	vl	vl	vl	vl	vl	vl	vl	vl	l	l	h
1	vl	vl	vl	vl	vl	vl	vl	vl	vl	l	m

Table S2.3. Classification of the canyon type according to angles α and β

α(°)\β(°)	<15°	16°-30°	31°-45°	46°-60°	61°-80°	>81°
5.71°-11.30°	1a	1b	1c	1d	1e	1f
11.31°-21.80°	2a	2b	2c	2d	2e	2f
21.81°-30.96°	3a	3b	3c	3d	3e	3f
30.97°-38.65°	4a	4b	4c	4d	4e	4f
38.66°-45.27°	5a	5b	5c	5d	5e	5f
>45.28°	6a	6b	6c	6d	6e	6f

Table S2.4. Updated values for the accessibility sub-index (I_a)

Distance from roads (m)	Value
0-100	10
10 -200	9
201-300	8
301-400	7
401-500	6
501-600	5
601-700	4
701-800	3
801-900	2
>901	1

Table S2.5. Updated values for the penetrability sub-index (I_p)

Soil hardness (sh_i)	Slope (%) (s_i)	Aspect (e_i)	Pre-extinction trails (m/ha) (pt_i)	Assigned value
Hard	0–5	N	>46	10
	6–10	–	41–45	9
	11–15	NE	36–40	8
Moderately hard	16–20	NW	31–35	7
	21–25	E	26-30	6
Moderately loose	26–30	W	21–25	5
	31–35	SE	16–20	4
	36–40	SW	11–15	3
	41–45	S	6–10	2
Loose	>46	–	0–5	1

Table S2.6. Fireline opening sub index (I_p) values for the fuel difficulty and fire-line production for manual or mechanical tools by fuel type (Rodríguez y Silva et al. 2014)

Fuel model	Fuel difficulty weight (d_i)	Manual rate weight (m h^{-1})	Mechanical rate weight (m h^{-1})
P1[a]	10	10 (>46)	10 (>1801)
P2	10	10 (>46)	10 (>1801)
P3	10	10 (>46)	10 (>1801)
P4	10	10 (>46)	10 (>1801)
P5	10	10 (>46)	10 (>1801)
P6	10	10 (>46)	10 (>1801)
P7	9	9 (41–45)	9 (1601–1800)
P8	9	9 (41–45)	9 (1601–1800)
P9	9	9 (41–45)	9 (1601–1800)
PM1[b]	9	9 (41–45)	9 (1601–1800)
PM2	9	9 (41–45)	9 (1601–1800)
PM3	8	8 (36–40)	8 (1401–1600)
PM4	8	8 (36–40)	8 (1401–1600)
M1[c]	7	7 (31–35)	7 (1201–1400)
M2	7	7 (31–35)	7 (1201–1400)
M3	5	5 (21–25)	5 (801–1000)
M4	5	5 (21–25)	5 (801–1000)
M5	4	4 (16–20)	4 (601–800)
M6	5	5 (21–25)	5 (801–1000)
M7	3	3 (11–15)	3 (401–600)
M8	4	4 (16–20)	4 (601–800)
M9	3	3 (11–15)	3 (401–600)
HPM1[d]	8	8 (36–40)	8 (1401–1600)
HPM2	8	8 (36–40)	8 (1401–1600)
HPM3	8	8 (36–40)	8 (1401–1600)
HPM4	6	6 (26–30)	6 (1001–1200)
HPM5	6	6 (26–30)	6 (1001–1200)
HR1[e]	7	7 (31–35)	7 (1201–1400)
HR2	7	7 (31–35)	7 (1201–1400)
HR3	7	7 (31–35)	7 (1201–1400)
HR4	7	7 (31–35)	7 (1201–1400)
HR5	7	7 (31–35)	7 (1201–1400)
HR6	7	7 (31–35)	7 (1201–1400)
HR7	7	7 (31–35)	7 (1201–1400)
HR8	7	7 (31–35)	7 (1201–1400)
HR9	7	7 (31–35)	7 (1201–1400)
R1[f]	2	2 (6–10)	2 (201–400)
R2	2	2 (6–10)	2 (201–400)
R3	1	1 (<5)	1 (<200)
R4	1	1 (<5)	1 (<200)

a= grass models; b=grass & shrubs models; c=shrubs models; d=litter. Grass & shrubs under canopy models; e=litter under canopy models; f=slash models

Table S2.7. Adjustment coefficient depending on the slope for the fire-line construction sub-index (I_c)

Slope (%) (s_i)	Adjustment coefficient hand line $(SC_i)_{hl}$	Slope (%) (s_i)	Adjustment coefficient dozer line $(SC_i)_{Dl}$
0–5	1	0-5	1
6–10	1	6-10	1
11–15	1	11-15	1
16–20	0.8	16-20	0.8
21–25	0.8	21-25	0.7
26–30	0.8	26-30	0.6
31–35	0.6	31-35	0.5
36–40	0.6	-	
41–45	0.6	-	
>46	0.5	-	

Table S2.8. Slope penalty adjustment to final SDI output for non-burnable fuels

Slope (%)	Value
0-10	0.1
10 -20	0.2
20-30	0.4
30-40	0.6
40-50	0.8
> 50	1

Table S2.9. Large fires in Spain used to develop new fire propagation sub-indicies

Fire	Size	Year
Obejo	4,979 ha	2007
Mijas	1,705 ha	2011
Coín-Marbella	8,226 ha	2012
Quesada	9,760 ha	2015
Segura	687 ha	2017

S3: Case Study modeling inputs, statistical testing results, and example application

Table S3.1. FlamMap Parameters used for 97th percentile fire weather on the Jolly Mountain and Segura fires

Parameter	Jolly Mountain	Segura
Wind speed (mph/kph)	10/16	8/14
Wind direction (Deg.)	300	266
Wind Ninja grid size (m)	120	120
1 hr fuel moisture (%)	3	3
10 hr fuel moisture (%)	4	5
100 hr fuel moisture (%)	6	7
Herbaceous fuel moisture (%)	67	45
Woody fuel moisture (%)	92	79
Live fuel moisture (%)	100	85

Table S3.2. McNemar test results of the Jolly Fire. (tSDIor= Original), (tSDIupd= Updated), ctrl= fire perimeter controlled. unctrl= fire perimeter uncontrolled.

(tSDIor-tSDIupd) ctrl	p-value	(tSDIor-tSDIupd) unctrl	p-value
Very low	1.525E-100	Very low	3.2818E-34
Low	3.378E-33	Low	1.365E-17
Medium	6,981E-11	Medium	4.725E-66
High	1.0371E-4	High	3.597E-46
Very high	2.183E-101	Very high	0.774

Table S3.3. McNemar test results of the Segura Fire. (SDIor= Original), (SDIupd= Updated), ctrl= fire perimeter controlled. unctrl= fire perimeter uncontrolled.

(SDIor-SDIupd) ctrl	p-value	(SDIor-SDIupd) unctrl	p-value
Low	0,016	Low	0,022
Medium	2.810E-7	Medium	8.006E-4
High	1.038E-27	High	3.902E-16
Very high and Extreme	9.293E-38	Very high and Extreme	5.185E-12

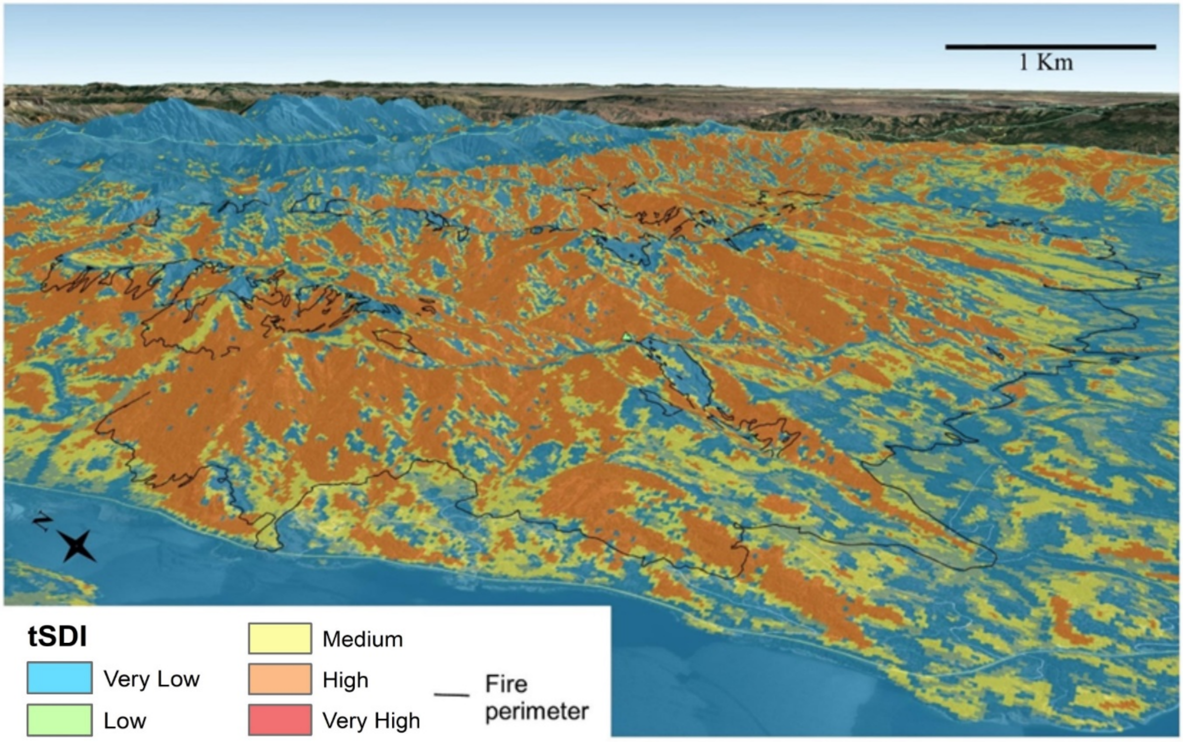

Figure S3. Screen capture of tSDI Google Earth overlay, Jolly Mountain Fire, Okanagan-Wenatchee National Forest, USA, August 29, 2017. Products developed in ArcGIS were converted to Google Earth KMZ format at the request of fire managers. SDI overlays were used by incident management team operations personnel to assess the relative difficulty in completing a range of possible tactical fire management operations.

S4: Updating Ice calculations to account for more severe fire weather

Here we present an "energy behavior update factor" (Δ) that can be used to calculate I_{ce} values under more severe fire weather conditions than used from historical databases. The equations presented below were developed by Rodríguez y Silva for application in Spain. Note that applications in the U.S. ran FlamMap using observed and forecasted weather, rather than historical weather data, such that such updates were unnecessary.

$\Delta = 1 + (\mu_f - \mu_i)$

(S3.1)

$\mu_f = 0{,}896713 + 0{,}00558901 \cdot T_f + 8{,}65159x10^{-5} \cdot H_f + 0{,}0021835 \cdot V_f$ R^2 =0,994(S3.2)

$\mu_i = 0{,}896713 + 0{,}00558901 \cdot T_i + 8{,}65159x10^{-5} \cdot H_i + 0{,}0021835 \cdot V_i$

(S3.3)

The components of the "energy behavior update factor" (Δ), are temperature (T) ºC, humidity (H) (%) and wind speed (V) km/h. T_f, H_f, V_f, represent the new weather conditions and T_i, H_i, V_i, represent the historical data weather conditions that were considered to calculate the energy behavior sub-index. The (I_{ce}) update to the new weather conditions will be $\Delta \cdot I_{tce}$.